Transition Moments of Visible Region Absorption Bands of *trans*(*Cl*)-Triammineaquadichlorocobalt(Ⅲ) Chloride

Yoshihiro Mitsutsuka,*,# Nobuhiko Nawa,## Shuji Yoshizawa,# Hirofumi Yajima,† Keiji Iriyama,†† Hisao Hidaka,### and Masamichi Tsuboi†††

Department of Chemistry, Department of Physics, and Frontier Research Center for the Global Environment Protection, Meisei University, 2-1-1, Hodokubo, Hino, Tokyo 191-8506

†Department of Applied Chemistry, Tyoko University of Science, 1-3 Kagurazaka, Shinjuku-ku, Tokyo 162-8601

††Institute of DNA Medicine, Jikei University, 3-25-8 Nishi-Shinbashi, Minato-ku, Tokyo 105-8461

†††College of Science and Engineering, Iwaki-Meisei University, Iwaki, Fukushima 970-8551

(Received April 16, 2002)

From single crystals of *trans*(*Cl*)-$[CoCl_2(NH_3)_3(H_2O)]Cl$, thin sections with different orientations and different thicknesses were prepared, and their polarized absorption spectra were examined in the 350–850 nm region using a microspectrophotometer. Two absorption peaks, caused by the ($x^2-y^2 \leftarrow xy$)-type transitions of the d-electrons of Co, were found: a 15750 cm^{-1} peak was assigned to overlapping $A_2 \leftarrow A_1$ and $B_2 \leftarrow A_1$ type transitions of the complex ion with C_{2v} symmetry; a 19210 cm^{-1} peak was assigned to a $B_1 \leftarrow A_1$ type transition. The molar extinction coefficients (ε) were determined at each of these peaks: $\varepsilon(\|c) = 104$ and $\varepsilon(\perp c) = 16$ l cm^{-1} mol^{-1} at 15750 cm^{-1}, and $\varepsilon(\|c) = 5$ and $\varepsilon(\perp c) = 54$ l cm^{-1} mol^{-1} at 19210 cm^{-1}. These ε values were explained by taking distortions of the d-electron orbitals into consideration, that are partly caused by the oxygen atom coordination and partly by some vibronic couplings between the d-electron orbitals and cobalt-ligand stretching vibrations.

The subject of this study was a *trans*(*Cl*)-triammineaquadichlorocobalt(Ⅲ) ion, $[Co^{Ⅲ}Cl_2(NH_3)_3(H_2O)]^+$, (Fig. 1[I]). This is an interesting complex ion; its chloride is readily brought into a single crystal, and the crystal shows a marked dichroism. This crystal is called a dichro chloride crystal throughout this paper. We attempted to examine the optical anisotropy of this crystal in detail so as to develop a deeper insight into the background of the dichroism. Specifically, it appeared to be mysterious[1] why its lowest frequency band at 635 nm (15750 cm^{-1}) does not split into two, and why it seems to be unusually strong. A quantitative set of data on the optical anisotropy would solve such a mystery.

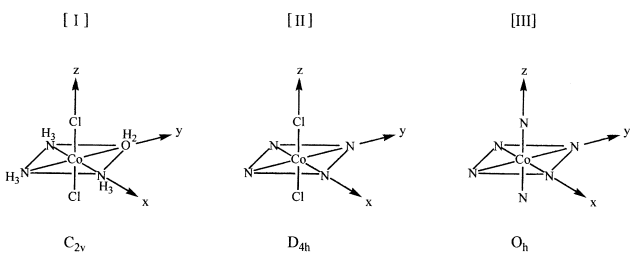

Fig. 1. Molecular structure of *trans*(*Cl*)-triammineaquadichlorocobalt(Ⅲ) cation [I]. Other two related Co(Ⅲ) cations with higher symmetries [II and III].

It is now well established that the visible-region absorption band of an octahedral cobalt complex, with O_h symmetry (Fig. 1[III]) is caused by three ($x^2 - y^2 \leftarrow$ xy)-type transitions of its d-electrons. The orbitals relevant to these electronic transitions are schematically shown in Fig. 2. Here, the excited states (ξ, η, and ζ) have the same energy as one another; this triply degenerate state is named T_{1g}, after its symmetry species.

When the two meridional nitrogens are replaced by chlorine anions (as shown in Fig. 1[II]), and the symmetry of the ion is brought into D_{4h}, the orbitals in the ξ, η, and ζ states must be distorted. It is known that the ζ state (now A_{2g} of D_{4h}) now has a slightly higher energy than the other two, while ξ and η still have the same energy as each other (doubly degenerate E_g state).

On going one step further, let us replace one of the four nitrogens by oxygen (Fig. 1[I]) to construct the complex ion now in question. Here, the orbitals of the ξ, η, and ζ states must be further distorted. The symmetry of the ion is now C_{2v}. An elucidation of the characteristic optical property of this complex caused by such a distortion was the target of this study.

For our optical measurement, we chose a single crystal of chloride of this ion as a sample. The structure of this crystal was determined by Y. Tanito et al[2]; it is a hexagonal crystal, and the ions in it are arranged with their Cl–Co–Cl lines all parallel to the *c*-axis. Thus, it looked promising that a proper investigation into the optical properties of this crystal should lead to a piece of information relevant to our present aim.

Department of Chemistry, Meisei University.
Department of Physics, Meisei University.
Frontier Research Center, Meisei University.

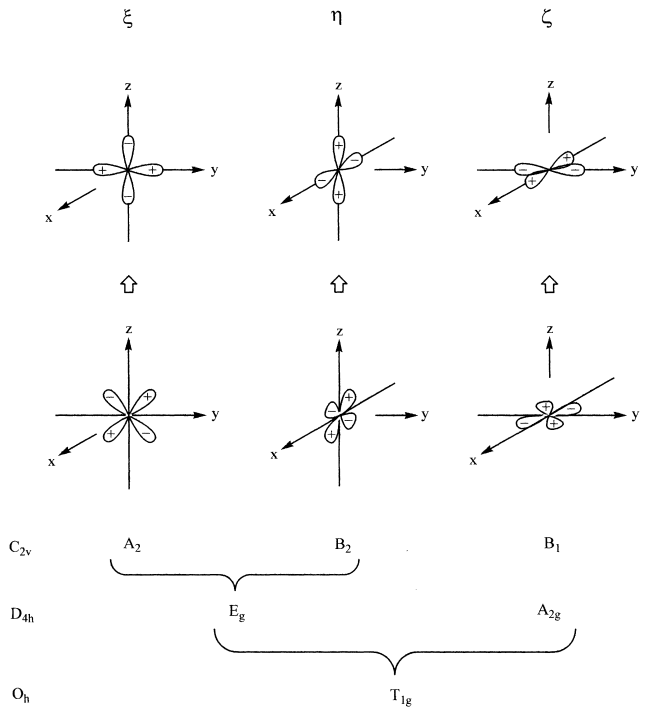

Fig. 2. Schematic illustration of the d-electron orbitals involved in the lowest electronic excitation of octahedral Co complex ion.

With this expectation in mind, we have developed a general method to prepare thin crystal sections with the desired orientations and thicknesses, and also a general method for calculating the intrinsic molar extinction coefficients from the experimental absorbance data. Because these methods are useful, not only for studying the crystal now in question, but also for studies of other various crystals in the future, they are also described below.

Experimental

Preparation of the Complex. First, a triamminetrinitrato complex $[Co(NO_3)_3(NH_3)_3]$ was prepared according to the Birk[3] and Jørgensen[4] procedures. By treating this trinitrato complex with hydrochloric acid, dichro chloride, *trans*(*Cl*)-$[CoCl_2(NH_3)_3(H_2O)]Cl$, was obtained according to a method reported by Meyer, Dirska, and Clementz[5] and Jørgensen.[6] Anal. Calcd for $[CoCl_2(NH_3)_3(H_2O)]Cl$: Co, 25.2; Cl, 45.4; NH_3, 21.8%. Found: Co, 25.0; Cl, 44.6; NH_3, 21.4%.

Preparation of Thin Crystal Sections. The used dichro chloride crystals were grown by the slow evaporation of a dilute solution in HCl (0.1 mol/L) while keeping the temperature at 25 ± 2 °C. The size of a crystal was typically 0.3 × 0.3 × 0.7 mm, and the crystals were found to be very soft and brittle. Each single crystal was embedded into a block of poly(methyl methacrylate) resin (Technovit 4004 cold curing resin, Heraeus) at room temperature. The resin piece including the crystal was then sawed by a diamond saw (850 wire saw, South Bay Technology) to produce a desired plane of the crystal. This plane was then ground and polished flat using successively finer material. Various grades of carborundum, alundum, or cerium(IV) oxide flour were used together with kerosene or ethanol as a lubricant for the grinding and specular polishing. The polished surface of the resin piece was cemented with epoxy resin to a glass slide, and the other side of the cemented piece was also ground to the desired thickness and then polished. The thickness of the crystal plate was determined with a VF7500 Keyence measurement microscope.

Microspectrophotometer. A computer-controlled double-beam microspectrophotometer was constructed from a Jasco SS50C monochromater, an Ushio intense light source (300 W I_2 lamp) and an optical microscope equipped with a pair of MO30X Olympus reflecting objectives. The monochromated light was collimated with spherical mirrors and passed through a Glan polarizer prism (PLG15, Bernhard Holle Nachfl., the extinction ratio: 10^{-5}) which was rotatable with a computer-controlled stepping motor. The light from the prism was split into reference and sample beams with a mirror chopper. The sample beam was focused onto a crystal plate of the complex with a reflecting objective (Fig. 3). The objective consisted of a concave mirror with a diameter of 28 mm and a convex mirror with a diameter of 5 mm. The size of the focus was 150 × 150 μm, and the area could be reduced depending on the shape and dimensions of the sample specimen, if needed, by placing a diaphragm. The emergent light from the sample plate was collected with another reflecting objective on a R3896 Hamamatsu photomultiplier. The reference beam was balanced by adjusting an attenuator and focused onto the same photomultiplier. The spectra were measured from 350 to 850 nm with polarized light having orthogonal electric vector directions at

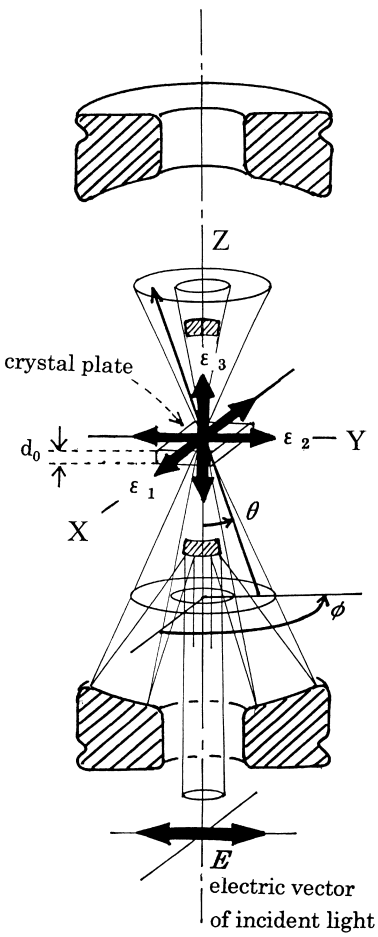

Fig. 3. Passage of light through crystal plate placed between reflecting objectives (MO30X).

the absorption maximum and minimum of the band peak.

Results and Discussions

1. Polarized Spectra of Thin Crystal Sections. First, we confirmed whether the crystal in hand was the same as that which was subjected to a previous X-ray crystallographic study by Tanito et al.[2] We found that our crystal was hexagonal with unit-cell dimensions of $a = 7.294$ Å and $c = 8.665$ Å, which were exactly equal to what were found previously.

Each sample crystal which we used had an outside appearance as shown in Fig. 4. Its length along the *c*-axis was about 0.7 mm and about 0.3–0.5 mm along the two perpendicular directions. For convenience, the *a*- and *b*-axes were defined while referring to this particular crystalline habit, as shown in Fig. 4.

A 10 μm thick section perpendicular to the *c*-axis was first prepared (Fig. 5(a)), and its absorption spectra were recorded with the incident light polarized along the *a*- and *b*-axes. As shown in Fig. 5(a), the $\|a$ and $\|b$ spectra came out practically identical with each other. This was just what was expected for a uniaxial crystal. Thus, this result was taken as indicating the validity of the present experimental setup and procedure.

In a similar manner, bc and ca sections of the crystal were prepared and their polarized absorption spectra were recorded. The results are shown in Figs. 5(b) and (c). For every case, two absorption peaks were found at 15750 and 19210 cm^{-1}.

2. Molar Extinction Coefficients. From these observed curves, we attempted to evaluate the molar extinction coefficient at each observed absorption peak.

To minimize the errors in the thickness measurements of the sections, the absorbance observed at each absorption peak was plotted against the experimentally determined thickness (Fig. 6). Every plot gave a nearly straight line, passing the origin; the average absorbance value for a section with a thickness of 10 μm was determined with an error of less than 0.01 μm. The absorbance values normalized to 10 μm thickness in this way are given Table 1.

Next, we needed to take the inclination of the beam into account. The beam direction was given by Eulerian angles θ and ϕ in an XYZ rectangular coordinate system fixed on a sample crystal (Fig. 3). As can be seen in Fig. 3, the bundle of beams passing the sample was a solid body formed by two coaxial cones whose apex angles were θ_1 (inside) and θ_2 (outside). To define a few more parameters, let us refer to Fig. 3 again. Suppose that the sample crystal has three molar extinction coefficients (ε_1, ε_2, and ε_3) for light polarized along X, Y, and Z, respectively. Suppose, in addition, that the incident light is polarized along Y, and therefore ε_1 is not relevant at all in this case.

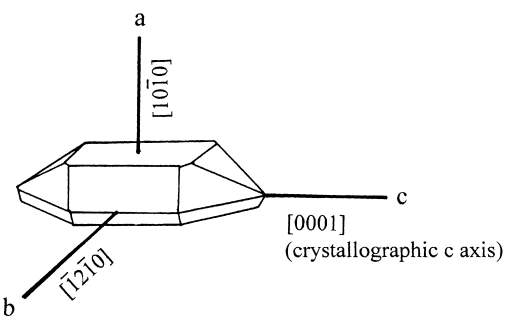

Fig. 4. Crystal shape of dichro chloride and the coordinate system.

We now derive a general relation between an observed absorbance value and the intrinsic molar extinction coefficients (ε_2 and ε_3):

$$\text{Observed absorbance} = -\log\frac{\int_{\theta_1}^{\theta_2}\sin\theta\int_0^{2\pi}10^{-\varepsilon cd}\,d\phi\,d\theta}{\int_{\theta_1}^{\theta_2}\sin\theta\int_0^{2\pi}d\phi\,d\theta}, \quad (1)$$

$$\varepsilon = \varepsilon_2\frac{1}{1+\tan^2\theta\cos^2\phi} + \varepsilon_3\frac{\tan^2\theta\cos^2\phi}{1+\tan^2\theta\cos^2\phi}, \quad (2)$$

$$d = \frac{d_0}{\sqrt{1-\sin^2\theta\left(\frac{\sin^2\omega}{{n_2}^2}+\frac{\cos^2\omega}{{n_3}^2}\right)}}, \quad (3)$$

and ω is defined as

$$\omega = \tan^{-1}(\tan\theta\sin\phi). \quad (4)$$

Here, c is the concentration of the molecule in the crystal, d_0 is the observed thickness of the section, and n_2 and n_3 are the refractive indices of the sample crystal for the light polarized along Y and Z axes (corresponding to ε_2 and ε_3, respectively).

For our present case of dichro chloride, the following parameters are proper: $\theta_1 = 11°$, $\theta_2 = 23°$, $d_0 = 10$ μm, $c = 8.07$ mol/L, $n_a = n_b = 1.70 \pm 0.01$, and $n_c = 1.84 \pm 0.01$. Here, the refractive indices (n_a, n_b, and n_c) were determined by ourselves using an immersion method.[7] By using Eqs. 1, 2, 3 & 4 and the absorbance values given in Table 1, the values of the molar extinction coefficient were determined. The results are given in Table 2.

3. Comparison of the Transition Moments of the D_{4h} and C_{2v} Complexes. In Fig. 7a, a set of ε (molar extinction coefficient) versus frequency (cm^{-1}) curves of *trans*(*Cl*)-$[CoCl_2(NH_3)_3(H_2O)]$ ([I] in Fig. 1) are shown. This is a summary of the present experimental results. Along with this, a similar set of the curves of *trans*-$[CoCl_2(en)_2]ClO_4$ ([II] in Fig. 1) is given based on R. Dingle's work[8] (see Fig. 7b). The two cobalt complex ions ([I] and [II]) are different in only one coordinating atom, N versus O. Nevertheless, marked differences are found in the ε/cm^{-1} curves, both in the peak positions and the peak intensities. Thus, [I] gives two peaks at 15750 and 19210 cm^{-1}, whereas [II] gives a peak at 16150 and a shoulder at about 22000 cm^{-1}. It is even more prominent that the ε values are much higher for [I] than for [II].

4. Transition Frequencies In general, the energy of a ($x^2 - y^2 \leftarrow xy$) type d-electronic transition is given by

$$(1/4)\{\delta(L_1) + \delta(L_2) + \delta(L_3) + \delta(L_4)\},$$

where $\delta(L_n)$ is the energy of the transition when all coordination sites in the orbital plane are occupied by the same four L_n ligands; hence, (1/4) $\delta(L_n)$ is the contribution to the transition

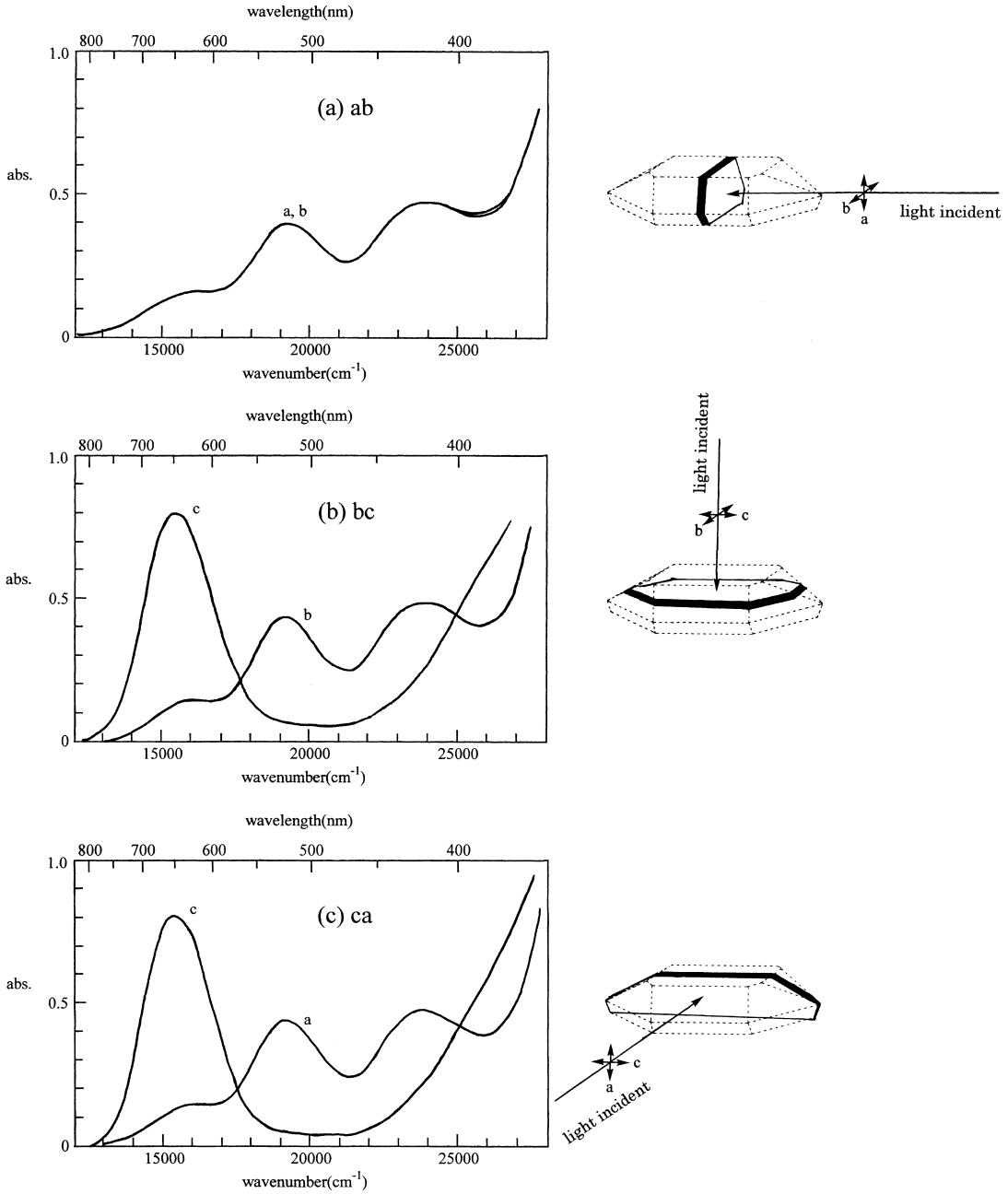

Fig. 5. Polarized absorption spectra for three sections of a single crystal of dichro chloride. (a) A thin section prepared along the crystallographic *ab* plane. (b) A thin section prepared along the crystallographic *bc* plane. (c) A thin section prepared along the crystallographic *ca* plane. How each section was cut from the crystal is illustrated on the right side of each spectrum.

energy from the n'th ligand, L_n. Therfore, the energies for the $x^2 - y^2 \leftarrow xy$, $y^2 \leftarrow z^2 \leftarrow yz$, and $z^2 - x^2 \leftarrow zx$ transitions can be represented by

$$(1/4)\{\delta(L_{+x}) + \delta(L_{-x}) + \delta(L_{+y}) + \delta(L_{-y})\},$$

$$(1/4)\{\delta(L_{+y}) + \delta(L_{-y}) + \delta(L_{+z}) + \delta(L_{-z})\},$$

and $(1/4)\{\delta(L_{+z}) + \delta(L_{-z}) + \delta(L_{+x}) + \delta(L_{-x})\}$, respectively,

where $\delta(L_q)$ is a parameter for the ligand located on the q-axis.

The appropriate values of δ were obtained for *trans*(*Cl*)-type complexes, as reported in a previous report:[8] $\delta(NH_3) = 21300\,cm^{-1}$, $\delta(Cl^-) = 10690\,cm^{-1}$, and $\delta(H_2O) = 12530\,cm^{-1}$. Thus, for [I], the frequencies of the transitions to the ξ, η, and ζ states (see Fig. 2) are expected to be 13800, 16000, and 19110 cm^{-1}, respectively. The actually observed peak at 15750 cm^{-1} is assignable to two unresolved transitions at 13800 and 16000 cm^{-1} (namely, $\xi + \eta$); the observed peak at 19210 cm^{-1} is assignable to the predicted 19110 cm^{-1} (ζ) transition. For [II], on the other hand, the frequencies to the states are expected to be 16000 (doubly degenerated) and 21300 cm^{-1}.

5. Symmetry-Allowed Electronic Transitions. Table 3 is a list of characters of irreducible representations of the group

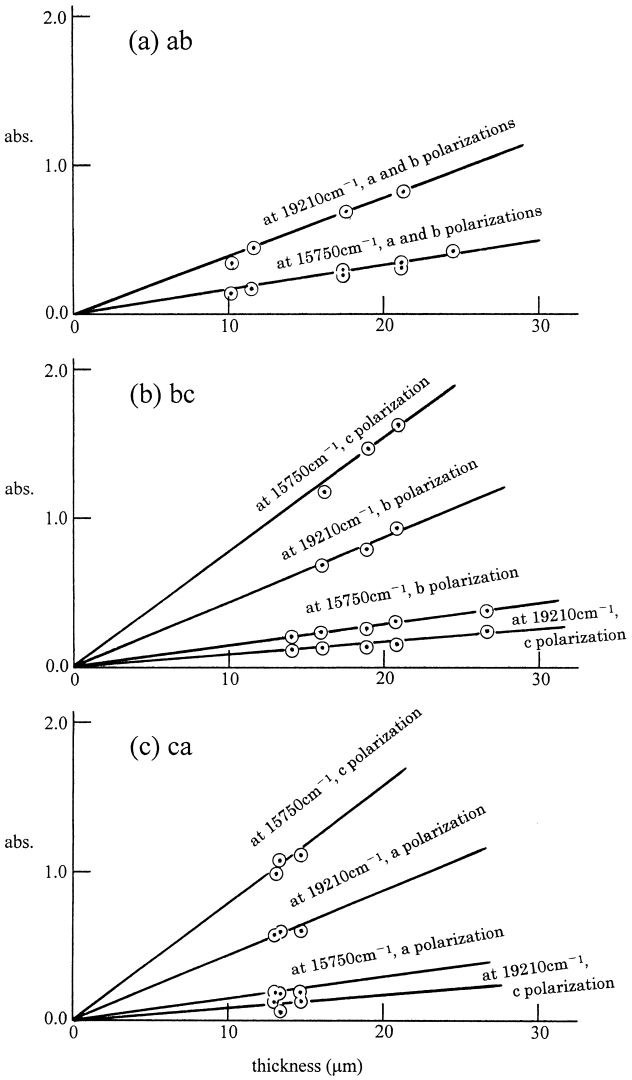

Fig. 6. Thickness-absorbance plots at the band peaks of dichro chloride crystal.

Table 1. Observed Absorbance for the Dichro Chloride Crystal Section with the Thickness of 10 μm

Spectrum	Polarization Direction	Absorbance at 15750 cm^{-1}	Absorbance at 19210 cm^{-1}
Ab	*a*	0.17	0.39
	b	0.17	0.39
bc	*b*	0.14	0.44
	c	0.79	0.09
ca	*c*	0.80	0.16
	a	0.10	0.45

Table 2. Molecular Extinction Coefficient (cm^{-1} mol^{-1})

	at 15750 cm^{-1}	at 19210 cm^{-1}
ε_a	16	54
ε_b	104	5

C_{2v}. Note that it is slightly different from the usual character table. Usually, the C_2 axis is assigned to z, whereas here it is assigned to y. This is done so as to make the coordinate system

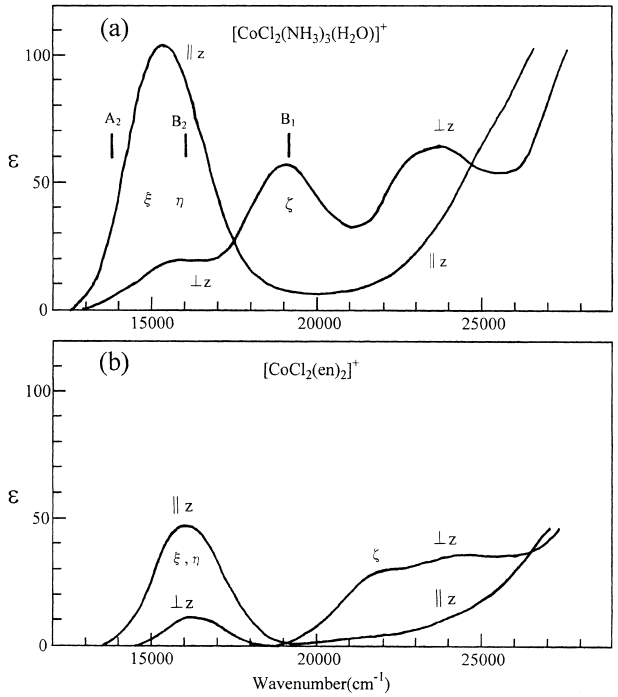

Fig. 7. Molar extinction coefficients (ε) of (a) $[CoCl_2(NH_3)_3(H_2O)]^+$ ion ([I] in Fig. 1) and (b) $[CoCl_2en_2]]^+$ ion ([II] in Fig. 1). The *xyz* coordinate system is defined as Fig. 1.
$\|z$: Electric vector of the incident light is along the Cl–Co–Cl line.
$\perp z$: Electric vector of the incident light is perpendicular to the Cl–Co–Cl line.

xyz for ion [I] consistent with what was chosen for ion [II] (see Fig. 1). For both ions, the Cl–Co–Cl direction is now assigned to z.

The table shows that an electronic transition, $B_2 \leftarrow A_1$ of [I], is allowed, and that its transition moment must be along z. In contrast, the corresponding one of the two transitions, $E_g \leftarrow A_g$, of [II] is forbidden (Table 4). Thus, it is now understandable that ε_c of [I] at 15750 cm^{-1} is much greater than ε_c of the corresponding peak at 16150 cm^{-1} of [II]. As can be seen in Table 3, another electronic transition, $B_1 \leftarrow A_1$ of [I], must also be allowed, and it should give a transition moment along x. This is assignable to ε_a observed for [I] at 19210 cm^{-1}. This is also greater than ε_a of [II] at 22000 cm^{-1}, which corresponds to an electronically forbidden transition.

6. Vibronic Coupling. It is now well known that many symmetry-forbidden d-electronic transitions of cobalt complex ions are actually observed, and that these are mostly attributed to proper vibronic couplings. For our present case of $[CoCl_2(NH_3)_3(H_2O)]$-ion, a number of electronically forbidden transitions are also observed, and therefore vibronic couplings must be taken into consideration.

Let us assume that the $[CoCl_2(NH_3)_3(H_2O)]$-ion is a 7-atom system having Co, two Cl's, three (NH_3)'s, and one (H_2O), because normal vibrations made up by the movements of the hydrogen atoms would not be involved in the vibronic couplings with the d-electrons. The number of normal vibrations of such system is $3 \times 7 - 6 = 15$, and are classified as shown in the

Table 3. Symmetry Types (Species) and Characters for the Point Group C_{2v}

C_{2v}	I	$C_2(y)$[a]	$\sigma(xy)$	$\sigma(yz)$		Number of normal vibrations of each type in the $CoCl_2(NH_3)_3(H_2O)^+$ ion[b]
A_1	+1	+1	+1	+1	y	6
A_2	+1	+1	−1	−1		1
B_1	+1	−1	+1	−1	x	4
B_2	+1	−1	−1	+1	z	4

a) C_2 axis is along y, instead of z. (see Fig. 1) b) (NH_3) and (H_2O) are assumed to be "atoms" instead of atomic groups.

Table 4. Symmetry Species of Electronic and Vibronic Excited States of d-Electrons in some Co Complexes

Excited state[a]			ξ	η	ζ
O_h				T_{1g}	
D_{4h}	Electronic			E_g	A_{2g}
	Vibronic[b]	x, y		$2A_{2u} + B_{1u}$	$3E_u$
		z		$3E_u$	no
	Observed ε[c]	x, y		12	~30
		z		51	~ 4
C_{2v}	Electronic		A_2	B_2	B_1
			forbidden	$\|\|z$	$\|\|x$
	Vibronic[b]	$\|\|x$	$4B_1$	$1A_2$	$6A_1$
		$\|\|y$	$1A_2$	$4B_2$	$4B_1$
		$\|\|z$	$4B_1$	$6A_1$	$1A_2$
	Observed ε[c]				
		x, y	16		54
		z	104		5

a) See Fig. 2. b) Vibrations that can cause allowed vibronic transitions and the numbers of such vibrations are given. c) Unit: cm^{-1} mol^{-1}

last column of Table 3.

Let us now consider, for example, the electronic excited state ξ of ion [I]. This eigenfunction belongs to symmetry species A_2 of C_{2v} and, therefore, the $\xi \leftarrow$ (ground state) transition is optically forbidden. Let us now construct a vibronic eigenfunction which is the product of the ξ function and an (A_2 vibrational eigenfunction). This should belong to a symmetry species given by the direct product $A_2 \times B_2 = B_1$. Here, the $B_1 \leftarrow$ (ground state, A_1) transition is now an allowed one, and should give a transition moment along x.

In Table 4, the symmetry species of the normal vibration that can cause a distortion of the d-electron orbital to result in an allowed vibronic transition is given for every electronic transition. The number of such normal vibrations is also given there; this number may be nearly proportional to the amount of the vibronic contribution of the observable transition moment. As can be seen in Table 4, the vibronic contributions to the transition moments along z and along $x + y$ are expected to be nearly equal (10/10) to each other at 15750 cm^{-1}. Therefore, the observed great ε_c value cannot be attributed to vibronic couplings. It must be due to a purely electronic transition moment. At 19210 cm^{-1}, on the other hand, the vibronic contribution is expected to be much greater than the transition moment perpendicular to z, the transition moment along z (10/1). The actually observed ε_c is very small, and ε_a (= ε_b) is much greater. This experimental result is now explained based on both purely electronic and vibronic distortions of the d-orbitals of the ζ excited state.

Conclusions

The marked dichroism of the [$CoCl_2(NH_3)_3(H_2O)$]Cl crystal is caused by a strong absorption band at 635 nm, whose transition moment is directed along the crystallographic c-axis. This corresponds to an electronically allowed $B_2 \leftarrow A_1$ transition of the complex ion with C_{2v} symmetry. The observed molar extinction coefficient ε_c is as great as 104 l cm^{-1} mol^{-1}, in contrast to the much smaller ε_c value found for *trans*-

$[CoCl_2(en)_2]ClO_4$ crystal (51 l cm^{-1} mol^{-1}). This difference is attributed to a distortion of the d-electron orbital in the plane perpendicular to the Cl–Co–Cl line, which is caused by replacing one of the four nitrogen atoms by oxygen.

As described in our previous paper,[1] this band was expected to split into two components, A_2 and B_2. This expectation was confirmed in the present study. Even in the present precise measurement, however, no piece of evidence of splitting was observed. It is now concluded that the two components happen to overlap perfectly with each other.

We thank Dr. Haruo Yamamoto of Meisei University for his technical support and valuable advice, especially on the preparation of thin crystal sections.

References

1 Y. Mitsutsuka, I. Kondo, and M. Nakahara, *Bull. Chem. Soc. Jpn.*, **59**, 2767 (1986).
2 Y. Tanito, Y. Saito, and H. Kuroya, *Bull. Chem. Soc. Jpn.*, **25**, 328 (1952).
3 E. Birk, *Z. Anorg. Chem.*, **175**, 409 (1928).
4 S. M. Jørgensen, *Z. Anorg. Chem.*, **5**, 185 (1894).
5 J. Meyer, G. Dirska, and F. Clementz, *Z. Anorg. Chem.*, **139**, 357 (1924).
6 S. M. Jørgensen, *Z. Anorg. Chem.*, **14**, 418 (1897).
7 E. M. Chamot and C. W. Mason, "Handbook of Chemical Microscopy," John Wiley & Sons, New York (1930), Vol. I, Chap. 11.
8 R. Dingle, *J. Chem. Phys.*, **46**, 1 (1967).